Origin of efficient light emission from a phosphorescent polymer/organometallic guest-host system

Raluca A. Negres, Xiong Gong, Jacek C. Ostrowski, Guillermo C. Bazan, Daniel Moses, and Alan J. Heeger*

Center for Polymers and Organic Solids, University of California, Santa Barbara, California 93106-5090, USA

(Received 5 February 2003; revised manuscript received 20 May 2003; published 29 September 2003)

Time-resolved photoinduced absorption measurements were performed at 77 K and room temperature on thin films of tris[9,9-dihexyl-2-(phenyl-4′-(-pyridin-2″-yl)fluorene]iridium(III) [Ir(DPPF)$_3$] doped into a blend of poly(*N*-vinylcarbazole) (PVK) with 2-(4-biphenylyl)-5-(4-tert-butylphenyl)-1,3,4-oxadiazole (PBD). We observe that in the PVK-PBD host blend, charge trapping (CT) plays an important role in the excited-state dynamics, in addition to exciplex formation and intensity-dependent decay of primary excitations. We develop a physical model which includes all interactions and which is in excellent agreement with the data. We find that 35% of the initial photoexcitation channels into CT states and that exciplexes are formed at a rate of 1/10 ps^{-1}. For the Ir(DPPF)$_3$ doped host composite, we write the rate equations for all population densities (which include the above excited-state species) and include energy-transfer rates from the host to the guest molecules. In both 0.2% and 2% Ir(DPPF)$_3$:(PVK-PBD) blends, Förster energy-transfer rates drop to half their low-temperature values at room temperature. We attribute this difference to a limited availability of guest molecules ready for energy transfer following charge trapping and insufficient spectral overlap due to shifts in the highest occupied and lowest unoccupied molecular orbital levels of the guest upon hole trapping. We conclude that the overall host-guest energy transfer is almost complete at room temperature in the 2% phosphorescent blend, with a large contribution (35%) from CT states which exhibit emission at all probe wavelengths.

DOI: 10.1103/PhysRevB.68.115209 PACS number(s): 78.66.Qn, 78.47.+p, 33.50.−j

I. INTRODUCTION

Phosphorescent dopants have been successfully used in organic light-emitting diodes (OLED's) to improve the device performance by breaking the spin conservation rule. The resulting harvesting of both singlet and triplet excitons has led to very high-efficiency OLED's.[1–13] One of the most promising guest-host systems uses the phosphorescent-guest tris[9,9-dihexyl-2-(phenyl-4′-(-pyridin-2″-yl)fluorene]iridium(III) [Ir(DPPF)$_3$, Fig. 1(a)] into a host blend comprising poly(*N*-vinylcarbazole) [PVK, Fig. 1(b)] with 2-(4-biphenylyl)-5-(4-tert-butylphenyl)-1,3,4-oxadiazole [PBD, Fig. 1(c)]. Because of the strong spin-orbit coupling of the heavy metal center, Ir complexes have efficient phosphorescence and short lifetimes, which typically range from 1 to 14 μs. In this study, we investigate in detail the physical processes involved in the high performance of Ir(DPPF)$_3$-doped OLED's. On a sub-nanosecond time scale, ultrafast pump-probe spectroscopy offers key information on how the photoexcitation is transferred from the polymer host to the organometallic phosphor guest.

When designing a host-guest system, one has to carefully analyze its ability to transfer the initial excitation (optical or electrical pumping) from the host material (''blue emitter'') to the dilute guest species which emit at longer wavelengths. The emission of the blend will be redshifted, with a twofold benefit: minimum reabsorption losses and tunable emission color with the use of various dopant chromophores. Often, the mechanism behind the observed photoluminescence (PL) spectra of polymer blends is the transfer of energy from host to guest via the long-range dipole-dipole interaction, known as Förster energy transfer.[14–16] As a result, complete, rapid energy transfer can occur even at dilute concentrations of the guest.[17,18] In electroluminescence (EL), following injection of the carriers, direct electron and hole trapping plays a role, and an excited dopant molecule is formed by the sequential trapping of a hole and then an electron onto the guest organometallic complex.

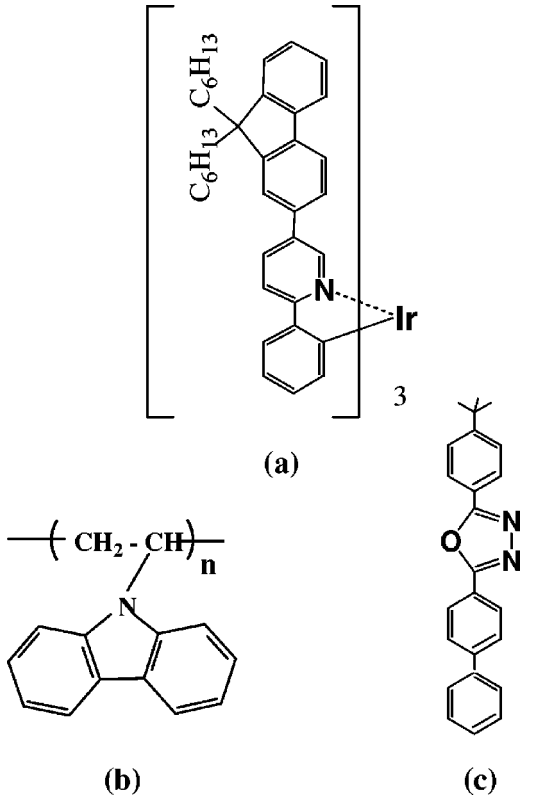

FIG. 1. Chemical structures of (a) Ir(DPPF)$_3$, (b) PVK, and (c) PBD.

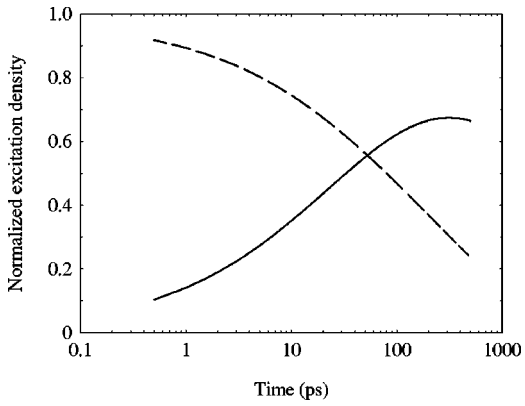

FIG. 2. Host (dashed line) and guest (solid line) normalized excited-state populations as function of probe time delay, at $T=77$ K and 2% doping concentration. Probe wavelength is 500 nm, while pump is set at 328 nm (see the details in Sec. III C).

Following ultraviolet (UV) optical pumping of the $Ir(DPPF)_3$:(PVK-PBD) blend, the observation of green phosphorescence at guest concentrations exceeding 0.1% proves that energy is indeed transferred from the host to the guest. For future device development based on such systems, techniques are required that go beyond steady-state experiments to quantify the rate and/or time scale of the energy transfer, and identify the mechanisms involved. By using the well-established sub-picosecond pump-probe method, it has been illustrated in the case of polymer blends[17] that during Förster energy transfer, the density of excited guest molecules increases as the concentration of excited host molecules decreases. Although the transfer mechanism is more complex, a similar picture can be presented for the $Ir(DPPF)_3$ system (Fig. 2). The details are described in Sec. III. A quick look at the dynamics of the phosphorescent blend, compared to that in fluorescent polymer blends, shows that the transfer proceeds somewhat more slowly ($\sim$200–300 ps) and the guest excitation reaches only about 70% of the initial host excitation.

II. EXPERIMENT

A. Sample preparation

The synthesis and characteristics of the phosphorescent $Ir(DPPF)_3$ have been reported elsewhere.[19] PVK and PBD were obtained from Aldrich and used without further purification. The organic thin films were spin cast at $\sim$1500 rpm from 3% solid solution in 1,2-dichloroethane onto UV grade fused silica substrates. In addition to PVK and PBD pristine films, and the PVK-PBD host (40 wt %), blends incorporating two concentrations of the guest molecule were prepared: 0.2 wt % and 2 wt %. Film thicknesses ranged from 200 nm to 300 nm (measured with Dektak profilometer). Visual examination showed that the films were of good optical quality (with the exception of PBD neat film where scattering centers form as a result of poor solubility).

B. Pump-probe instrumentation

The source for the ultrafast nonlinear spectroscopic measurements was a Spectra-Physics amplified Ti:sapphire system followed by an optical parametric amplifier, providing $\sim$120 fs [full width at half maximum (FWHM)] pulses at a repetition rate of 1 kHz with tunable wavelength. The pump wavelength was set at 328 nm (3.8 eV), close to the peak absorption of both PVK and PBD. The two host components absorb strongly, while the absorption from $Ir(DPPF)_3$ is much weaker. Although the extinction coefficients of the guest and that of the host at the pump wavelength have comparable values, the guest molecules are very dilute in the host composite ($\sim$1:350 molar ratio). Thus, the probability that an incident UV photon will be absorbed in the $Ir(DPPF)_3$ blend by either PVK or PBD is much higher. Transient absorption experiments were also performed in 2 wt % $Ir(DPPF)_3$:PMMA blends (PMMA is polymethylmethacrylate, a neutral polymer host with negligible absorption at 328 nm) in order to asses any possible contribution to the photoinduced absorption (PA) signal from directly excited guest molecules, in the absence of energy transfer from the host. Due to the dilute concentration of guest molecules in PMMA and despite their fairly large molar absorptivity at the pump wavelength (1.2×10^5 $cm^{-1}M^{-1}$), no PA signal was detected (2–3 % of pump absorption in the sample is a minimum requirement for a pump-probe experiment). Therefore, the number of guest molecules directly excited by the pump can be safely neglected throughout the paper. The pump energy was approximately 0.3 μJ per pulse with a spatial extent of 120 μm (HW1/eM) at the sample plane.

In order to probe the photogenerated excited state, the transmission of a femtosecond white-light continuum pulse (obtained by focusing 1 μJ of 800 nm into a 1-mm-thick sapphire window) was monitored. Wavelengths were selected from the continuum beam by using interference filters. We have performed measurements of the probe differential transmission at four different wavelengths, 480 nm, 500 nm, 532 nm, and 580 nm, in all thin-film samples throughout this work. The time delay of these single-wavelength probe beams, with respect to the pump pulse, was achieved with a computer controlled translation stage that is inserted into the pump beam path before the beam reaches the sample. The data presented in this work are expressed in terms of the differential change in transmission of the probe, dT/T, which is directly proportional to the change in absorption, $\Delta\alpha$, where $\Delta\alpha=\sigma N$, with σ the excited-state absorption cross section and N the excited-state population density. The 328-nm pump pulse caused a reduction in the transmitted intensity of the probe pulse (photoinduced absorption) at all wavelengths. In general, the PA signal decreases with time as a consequence of the decay of the excited-state population. The pump beam was mechanically chopped and phase sensitive (lock-in) detection was utilized to detect signals smaller than 10^{-2}. The samples were kept under dynamic vacuum to avoid photo-oxidation. Liquid-nitrogen cooling of the sample holder allowed us to perform experiments with the sample at $T=77$ K, in addition to room temperature. Experiments were performed within two days of spin casting the films to avoid phase separation (as observed in device studies).

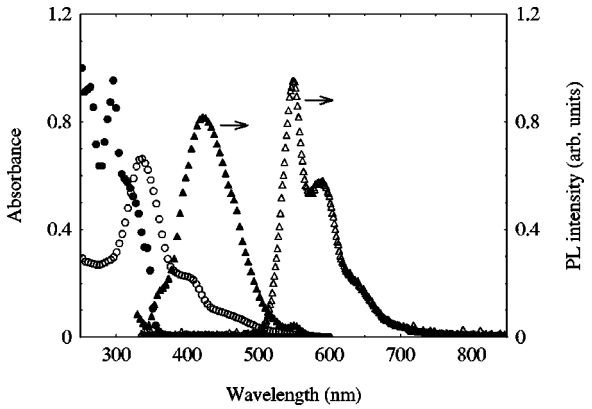

FIG. 3. Normalized absorption (● and ○) and photoluminescence (▲ and △) spectra of thin films of PVK-PBD (40 wt %) and $Ir(DPPF)_3$, respectively.

III. RESULTS AND DISCUSSION

As briefly noted in Sec. I, the energy-transfer mechanism in $Ir(DPPF)_3$:(PVK-PBD) blends is more complex than in the case of two-component polymer blends.[17,18] In order to maximize the spectral overlap of the host emission and the guest absorption for the desired Förster energy transfer, PVK was selected as the host because it is a blue emitter with emission spectrum that overlaps the absorption spectrum of the $Ir(DPPF)_3$. The UV-visible absorption and PL spectra of thin films PVK-PBD (40 wt %) and pristine $Ir(DPPF)_3$ are illustrated in Fig. 3. The requirement to have balanced charge injection in electroluminescent devices led to the addition of PBD into the host polymer since PVK is a hole-transport material while PBD is an electron-transport material.

The photoinduced absorption results obtained from the PVK-PBD host alone proved somewhat cumbersome. A simple model of single excited-state species with intensity-dependent dynamics (bimolecular annihilation), as is the case for poly(*p*-phenylene vinylene) (PPV) derivatives,[20–24] is not sufficient to account for the data obtained from the host material. The initial decay of the excited-state population at room temperature ($T=300$ K) seems to be too fast; an attempt to fit the data leads to an overestimated bimolecular decay rate, and the overall fitting curve is not in agreement with the data at longer time delays (the population has been depleted after the first 10 ps). This behavior suggests that only a fraction of the initial photoexcited species undergo bimolecular decay followed by natural decay dynamics, while the rest of the population lingers for a longer time. Considering the intrinsic properties of PVK[25] and PBD and previous work on charge-trapping (CT) states in conjugated polymer/fullerene blends,[21] we designed our experiments as follows: at a low enough temperature ($T=77$ K) the mobility of any carrier created upon excitation is zero, the carriers are frozen; we thus eliminate one mechanism that could contribute to the time evolution of the excited population in the host blend. This argument is well justified in amorphous polymers, such as PVK, where trap-controlled and dispersive hopping as transport mechanisms require an activation energy in excess of 0.1 eV.[25] Once we obtain all the parameters of the problem at this low temperature, we can later add in the CT contribution to the PA to explain the more complex behavior at room temperature.

A. PVK-PBD host at $T=77$ K

Interesting characteristics of the PL spectra from this host system have been recently discussed[26] in relation to the effect of carbazole-oxadiazole excited-state complexes on the efficiency of OLED's. While the PL maxima for PBD and PVK occur at 380 nm and 410 nm, respectively, the PL spectra of PVK-PBD blends (weight ratios from 95:5 to 40:60) show maxima at systematically longer wavelengths, near 425 nm (see Fig. 3). The redshift is essentially independent of composition and indicates the formation of an excited-state complex.

Two different classes of excited-state complexes, both important for polymer light-emitting diodes (PLED's), have been documented in the literature: *exciplexes* and *electroplexes*. Photoexcitation generates free carriers either directly($\sim 10\%$ in conjugated polymers), when the electronic wave functions are delocalized or when dissociation of neutral excited states is facile, i.e., when the exciton binding energy is small. Thereby, the emission signature of electroplexes is visible in the EL spectrum but not typically in the PL spectrum. Conversely, exciplexes are generated through photoexcitation, so their emission is visible in both EL and PL spectra. The presence of excited-state complexes in the host matrix alters the energy levels present, and may very well impact the efficiency with which energy can be transferred to the guest molecules.

Based on our observations, we propose a simple model to describe the time evolution of excited-state population in the PVK-PBD blends at $T=77$ K; the model incorporates the following species: (i) primary excitations with effective new parameters for both the bimolecular and the natural decay rates (independent from those in pristine films) and (ii) exciplexes with formation rate and lifetime yet to be determined, which exhibit PA (or stimulated emission) at longer probe wavelengths (redshifted with respect to pristine films of PVK and PBD).

The use of effective parameters for the primary excitations is a simplified approach to evaluating the composite host, as opposed to studying the individual components and including interactions between different molecular species in the blend. We made a quantitative attempt to follow the latter route where the ratio of PVK to PBD species along with their excited-state absorption cross sections need to be precisely determined. The quality of pristine PBD films (with a tendency toward crystallization) and other experimental errors prevented consistent results. Our data indicate that the bimolecular decay rate of PBD is greater than that in PVK (one order of magnitude) and the lifetime is shorter, 50 ± 10 ps (vs 1500 ± 100 ps in PVK).

Following the intensity-dependent dynamics of the excited-state absorption in PPV oligomers, we write a rate equation of the form[20–22]

$$\frac{dN_1}{dt}=-\frac{N_1}{\tau_1}-\frac{\beta_0}{\sqrt{t}}N_1^2, \tag{1}$$

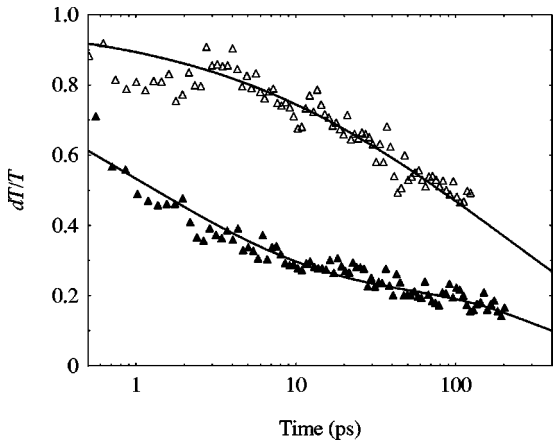

FIG. 4. The excited-state dynamics of PVK-PBD blend at 480 nm (△) and 532 nm (▲) ($T=77$ K). Fitting parameters in Eqs. (1) and (2) are given in the text.

where the first term represents the natural lifetime decay τ_1 and the second term describes the bimolecular decay β_0 arising from the interaction between excitations. The excitation densities and the mean separation between excitations encountered in our experiment (see Ref. 20) fall within the regime where Eq. (1) applies well.

The excited-state dynamics in the PVK-PBD blend for 480-nm probe are presented in Fig. 4 (open triangles). The best-fit parameters in the numerical integration of Eq. (1) (solid line) are the natural lifetime $\tau_1=1500$ ps and the bimolecular coefficient, $\beta_0(480\text{ nm})=6.9\times10^{-22}$ cm^3 ps$^{-1/2}$. The excitation density at the front surface, $N_0=\alpha F/\hbar\omega$, where F is the input fluence and α is the linear absorption coefficient at frequency ω, was 7×10^{19} cm$^{-3}\pm10\%$. The simple model of single excited-state species (primary excitations) undergoing intensity-dependent recombination dynamics [Eq. (1)] agrees quite well with the data at both 480 nm and 500 nm. Similar parameter values were inferred from our experiments in pristine PVK films. The results indicate that addition of PBD to the host material does not significantly influence the dynamics, at least at these particular wavelengths.

The situation is quite different at longer probe wavelengths, e.g., at 532 nm and 580 nm. The data suggest the presence of an additional excited species. From the PL spectra, we know that exciplexes are formed. PBD must play a role in the exciplex formation. If N_2 is the exciplex population, its dynamics can be described by

$$\frac{dN_2}{dt}=+\frac{N_1}{\tau_{exc}}-\frac{N_2}{\tau_2}, \tag{2}$$

where $(\tau_{exc})^{-1}$ and τ_2 are the rate of exciplex formation and lifetime, respectively. Equations (1) and (2) provide the correct model for fitting our data. Figure 4 also includes the more interesting dynamics of the blend at $T=77$ K and 532-nm probe (closed triangles). The bimolecular decay coefficient is found to be $\beta_0(532\text{ nm})=5.8\times10^{-21}$ cm^3 ps$^{-1/2}$, while $\tau_{exc}=10$ ps and $\tau_2=100$ ps. The large value for bimolecular decay points to the dominant signature of PBD at early times. After approximately 50 ps, excited PBD entities have already decayed, leaving behind longer-lived excited PVK species and exciplexes.

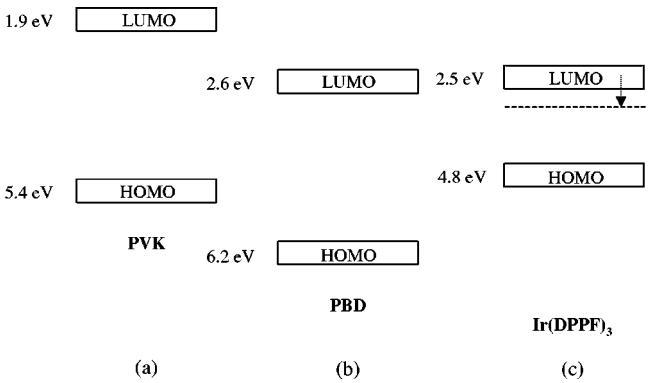

FIG. 5. HOMO and LUMO levels of (a) PVK, (b) PBD, and (c) Ir(DPPF)$_3$.

B. PVK-PBD host at $T=300$ K

We noted in the beginning of Sec. III that the behavior of the host blend at room temperature suggests the presence of longer-lived (up to milliseconds[27,28]) excited-state species. The upper limit on the time delay in our experiment was 0.5 ns, thus the contribution of metastable CT states will appear approximately constant over this time interval.

At this point, we have used a simple model, including primary excitations and exciplexes, to show the basic physical features that contribute to the population decay in our samples at $T=77$ K. In order to account for a constant term in the transient signal in the sub-nanosecond regime, we consider the excited-state absorption $\Delta\alpha$ to arise from a superposition of the remaining primary excitations N_1 and the newly formed CT states N_{CT}:

$$\Delta\alpha(t,\lambda)=N_1(t)\sigma_1(\lambda)+N_{\mathrm{CT}}(t)\sigma_{\mathrm{CT}}(\lambda). \tag{3}$$

The spectral dependence of each excited species i is determined by its cross section σ_i. The functional form of Eq. (3) is based on a physical model with the following features: (i) N_{CT} is formed at times within the experimental resolution ($\sim$200 fs);[28,29] (ii) the contribution of N_{CT} to $\Delta\alpha$ is approximately constant in the picosecond regime, i.e., $N_{\mathrm{CT}}(t)\equiv N_{\mathrm{CT}}$. The possibility of having CT states in the PVK-PBD host system is justified if we take a look at the highest occupied molecular orbital (HOMO) and lowest unoccupied molecular orbital (LUMO) levels of PVK and PBD[30] and their position with respect to each other [see Figs. 5(a) and 5(b)]. Both electron and hole trapping are favorable and we do not distinguish between them when we refer to the charge-trapping population N_{CT}.

Following closely the analytical treatment applied to conjugated polymer/fullerene bilayers and blends,[21] we first normalize the measured dT/T curve in the PVK-PBD blend at room temperature to the zero-delay value in the thin film at $T=77$ K (i.e., where CT states have been frozen) and rewrite Eq. (3) in the form

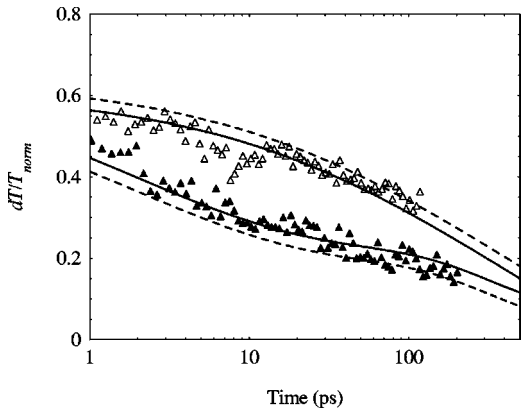

FIG. 6. Decay dynamics in PVK-PBD blend ($T=300$ K) for 480-nm (△) and 532-nm (▲) probes. The solid lines represent numerical fits from the model involving bimolecular decay of primary excitations, exciplex formation (at 532 nm), and a constant contribution from long-lived CT states (see the text). The dashed lines exclude the latter mechanism, analogous to the behavior observed at $T=77$ K.

$$dT/T_{norm}(t)=(1-\xi)g(t,\xi)+\xi\frac{\sigma_{\mathrm{CT}}}{\sigma_1}. \tag{4}$$

The decay function $g(t,\xi)$ in the first term of Eq. (4) is simply the nonlinear decay obtained by integrating Eq. (1) with the same parameters τ_1 and β_0 used to fit the dynamics of the excited-states N_1 in the previous case (Sec. III A). In the case of exciplex formation (observed at longer-wavelength probes), this term also includes the integration of Eq. (2). The dependence of this decay function on ξ, the charge-trapping probability, is included explicitly to indicate the sensitivity of the bimolecular decay to the fraction of excited states undergoing CT. The second term is time independent and contains the relative excited-state cross section of the CT states, $\sigma_{\mathrm{CT}}/\sigma_1$.

As shown in Fig. 6, this revised model yields good fits to the data at delay times beyond 1 ps. The two fitting parameters extracted from the fit are the fraction of CT states, $\xi=0.35\pm 9\%$, and the relative cross sections, $\sigma_{\mathrm{CT}}/\sigma_1=-0.081\pm 10\%$ and $0.092\pm 10\%$ (for 480-nm and 532-nm probes, respectively). We note that CT states have an emissive character at 480 nm while absorptive at 532 nm. All the other parameters, i.e., lifetimes and bimolecular rates, are fixed at their values determined in the preceding section.

C. Ir(DPPF)$_3$:(PVK-PBD) blend

At this point, we have developed a physical model which explains all the decay features observed in the PVK-PBD host, including the wavelength-dependent bimolecular decay, exciplex formation, and charge related phenomena (electron or hole trapping). Knowledge of the host dynamics is essential for subsequent modeling of the energy transfer to the guest molecules in the Ir(DPPF)$_3$ blend, the ultimate goal of this work.

Samples with two doping concentrations, 0.2% and 2%, were measured within two days of their preparation, under dynamic vacuum at liquid nitrogen and at room temperatures. The energy transfer is evident in the PL spectra (green emission from the guest molecules) at even lower doping levels.[12] Here we present results obtained with the 2% blend at both temperatures.

The HOMO and LUMO levels (solid boxes) of Ir(DPPF)$_3$ are shown in Fig. 5(c). The HOMO level was measured by cyclic voltammetry, the basic principle of which is to measure the oxidation potential of the compound. The LUMO level was calculated from the optical absorption assuming that the optical gap is equal to the energy gap (the HOMO-LUMO gap). A close look at these levels suggests the following scenario: (i) after initial excitation of PVK-PBD blend, a hole is trapped onto the guest organometallic complex (with the highest oxidation potential out of the three components), (ii) the presence of a positive charge on the metal center lowers the LUMO level (dashed line), and (iii) electron trapping by the cationic guest molecule is now feasible (it can be reduced more easily than the electron transport material) and energy transfer by Förster mechanism is affected as well (different overlap between the host emission and guest absorption). In other words, free carriers created by photoexcitation of the PVK-PBD blend end up being trapped on the iridium complex where they recombine within their lifetime ($\sim\mu$s).

The previous route, used in the host composite, to isolate different physical processes seems to be the logical route to follow in the Ir(DPPF)$_3$ blend as well. Namely, experiments conducted at $T=77$ K should solely reveal the dynamics of the energy transfer in the absence of mediated charge excitation. After the rate of transfer is determined, adding in CT states precisely follows the treatment from Sec. III B.

The coupled rate equations to model the Förster energy transfer between the host and the guest (subscripts H and G, respectively) are obtained from Eqs. (1) and (2) with the addition of one term:

$$\frac{dN_{1\mathrm{H}}}{dt}=-\frac{N_{1\mathrm{H}}}{\tau_{1\mathrm{H}}}-\frac{\beta_0}{\sqrt{t}}N_{1\mathrm{H}}^2-\frac{\beta_1}{\sqrt{t}}N_{1\mathrm{H}}, \tag{5a}$$

$$\frac{dN_{2\mathrm{H}}}{dt}=+\frac{N_{1\mathrm{H}}}{\tau_{exc}}-\frac{N_{2\mathrm{H}}}{\tau_{2\mathrm{H}}}-\frac{\beta_2}{\sqrt{t}}N_{2\mathrm{H}}, \tag{5b}$$

$$\frac{dN_{3\mathrm{G}}}{dt}=+\frac{\beta_1}{\sqrt{t}}N_{1\mathrm{H}}+\frac{\beta_2}{\sqrt{t}}N_{2\mathrm{H}}-\frac{N_{3\mathrm{G}}}{\tau_{3\mathrm{G}}}. \tag{5c}$$

The coefficients β_1 and β_2 measure the strength of the Förster transfer while $N_{3\mathrm{G}}$ denotes the guest population building up as the energy transfer proceeds. From fitting to the data, we find that the lifetime $\tau_{3\mathrm{G}}$ is greater than 10 ns, but an accurate determination within the time frame of our experiment is difficult. This observation is consistent with the long triplet lifetime of iridium complexes, on the order of few microseconds. The natural decay of the guest population during the first nanosecond will be neglected from here on. All other variables in Eqs. (5a)–(5c) have been defined in Sec. III A.

Equations (5a) and (5b) are valid for the host excited-state populations (primary excitations and exciplexes). Depending

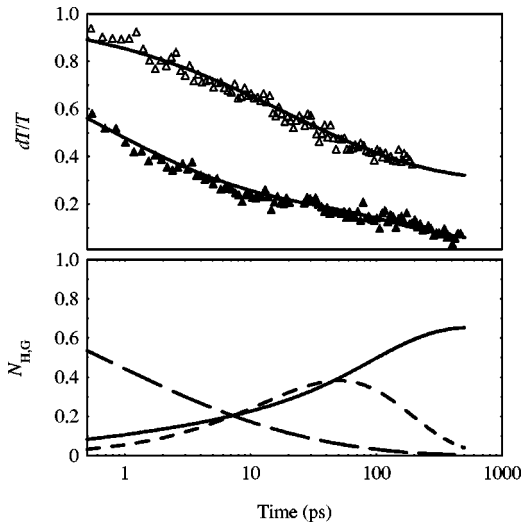

FIG. 7. Time-resolved Förster energy transfer in $Ir(DPPF)_3$:(PVK-PBD) blend (2 wt %, $T=77$ K). The probe beam was at 500 nm (△) and 532 nm (▲). The pump wavelength is 328 nm. Solid lines (top graph) represent fits using the excitation densities from Figs. 2 and 7 (bottom graph), respectively. Host population at 532 nm has two components, primary excitations and exciplexes (dashed and dotted lines, respectively), while the guest population is shown in solid line.

on the probe wavelength, one or both equations need to be used; i.e., at 480 nm and 500 nm, only Eqs. (5a) and (5c) apply, with the rate of energy transfer β_1. Subsequently, for numerical integration of Eq. (5c), only the first positive term contributes, $(\beta_1/\sqrt{t})\ N_{1H}$ while $N_{2H}\equiv 0$. At longer probe wavelengths, the entire set of Eqs. (5a)–(5c) is required for fitting the data. When all excited species are present, the differential change in transmission is obtained from the numerical integration of Eqs. (5a)–(5c) as follows:

$$dT/T(t)=dT/T(0)\left[N_{1H}(t)+N_{2H}(t)\frac{\sigma_{2H}}{\sigma_{1H}}+N_{3G}(t)\frac{\sigma_{3G}}{\sigma_{1H}}\right], \tag{6}$$

where $dT/T(0)=\sigma_{1H}N_0L$ with L-film thickness, and excited-state cross section σ_i's correspond to N_i's and $N_0=N_{1H}+N_{2H}+N_{3G}$ (initial excitation density).

In Fig. 7, we present data from the 2% $Ir(DPPF)_3$ blend at $T=77$ K, with 500-nm and 532-nm probes. The model provides excellent fits to the data. The energy transfer proceeds within a few hundreds of picoseconds. Note the slower transfer as compared to that in the earlier work on polymer blends, 300 ps vs 10 ps.[17,18] We attribute this difference to the strong mixing of ligand centered and metal-to-ligand charge transfer (MLCT) states due to spin-orbit coupling[31] that leads to a fairly weak oscillator strength of the MLCT state. The ability of the guest molecules to efficiently absorb the host emission in the dipole-dipole mediated energy transfer is diminished as well. For comparison, the rate of transfer in the 2% $Ir(DPPF)_3$ blend is at least five times smaller than that measured in polymer blends with similar doping, as discussed in Ref. 17.

In this work, the guest excitation reaches about 70% of the initial host excitation at all probe wavelengths (see Figs. 2 and 7) and $T=77$ K. This is expected since the number of excited guest molecules upon energy transfer depends on the pump pulse characteristics (in addition to other details such as the spectral features of the blend components) and is independent of the photon energy of the probe. This latter behavior provides an additional criterion for the adequacy of our model and fitting procedure, especially for the case of 532-nm probe where two species of the host population contribute to energy transfer, primary excitations N_{1H} (dashed line), and exciplexes N_{2H} (dotted line), respectively [see the bottom graph in Fig. 7 and Eqs. (5)]. The only fitting parameters used are the energy-transfer rates $\beta_{1,2}$ and the relative excited-state cross section σ_{3G}/σ_{1H} (see Table I).

Using the information and insights obtained from the 77-K data, we are finally ready to analyze the room-temperature excitation dynamics of the blends. Visual inspection of the blend under UV pump irradiation shows a significant change in brightness when the temperature is elevated from $T=77$ K to room temperature. We recall that CT species play an important role in the dynamics of PVK-PBD host. We already noted that, considering the HOMO and LUMO levels of the components, trapping of all the free carriers (following photoexcitation of the host) on the guest molecules is expected ($\sim$35% of initial population). It turns out that CT states in the Ir complex have an emissive character at all probe wavelengths (see Table I) and thus enhancement of the steady-state phosphorescence from the blend is expected with increasing temperature (green emission).

The physical model which takes the CT states into account was presented in the preceding section. We have ap-

TABLE I. Fitting parameters for numerical integration of Eqs. (1)–(6).

				PVK-PBD	$Ir(DPPF)_3$	$T=77$ K		$T=300$ K	
λ (nm)	σ_{1H} (10^{-17} cm^2)	σ_{2H}/σ_{1H}	σ_{3G}/σ_{1H}	σ_{CT}/σ_{1H}	σ_{CT}/σ_{1H}	β_1 ($ps^{-1/2}$)	β_2 ($ps^{-1/2}$)	β_1 ($ps^{-1/2}$)	β_2 ($ps^{-1/2}$)
480	2.78 [a]		0.55	−0.081	−0.133				
500	2.83 [a]		0.45	0	0	0.08 [b] (0.04 [c])		0.04 [b] (0.02 [c])	
532	4.99 [a]	0.15	0.15	0.092	−0.602		0.04 [b] (0.02 [c])		0.04 [b] (0.02 [c])
580	5.62 [a]	0.10	0.40	0.140	−0.535				

[a] ± 10% experimental errors.

[b] For 2% $Ir(DPPF)_3$ blend, at all wavelengths.

[c] For 0.2% $Ir(DPPF)_3$ blend, at all wavelengths.

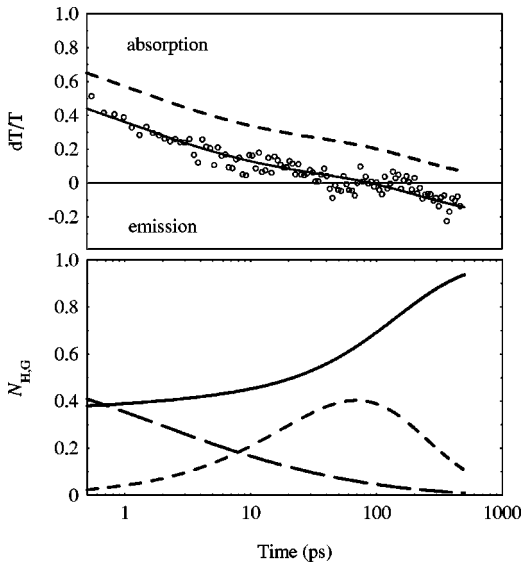

FIG. 8. Top: the excited-state dynamics of the 2% $Ir(DPPF)_3$ in PVK-PBD blend at $T=300$ K, probed at 532 nm (○). The solid and dashed lines are the fits obtained from numerical integration of Eqs. (5), with and without CT states, as explained in the text. Bottom: normalized host population densities, N_{1H} (dashed line) and N_{2H} (dotted line). Solid line shows the number of guest molecules excited by energy transfer and charge trapping.

plied it successfully to the $Ir(DPPF)_3$ blend at room temperature and the numerical fits are in good agreement with the data. Figure 8 shows the excited-state and population dynamics in the 2% blend at 532-nm probe and $T=300$ K. We note a few important features: (i) change in sign of the differential transmission from absorption in the host to emission of the guest, after ~100 ps, (ii) trapped charges on the dopant molecules largely contribute to the emission of the blend at early times (top graph, downward shift of the dotted line), (iii) 35% of the initial photoexcitation in the host being transferred to the guest is included in the population dynamics (bottom graph), i.e., normalized N_{1H} (dashed line) starts at 0.65 (zero time delay is not visible due to the logarithmic scale and fast initial decay of the population) while N_{3G} (solid line) begins at 0.35, and (iv) most noticeably, the guest excited population reaches close to 100% of the initial excitation in the host material at room temperature.

Experiments at all four probe wavelengths were also performed using the 0.2% $Ir(DPPF)_3$ blend (data not shown here). The results are consistent with those presented above. With the exception of the energy-transfer rate, which depends upon guest molecule concentration (i.e., mean distance between host and guest molecules), the same relative excited-state cross-section values were successfully used in fitting the data from both 0.2% and 2% blends.

All the fitting parameters for the various experimental conditions presented in this section are summarized in Table I. Two facts are worth noting from the table: (i) different excited-state species may be responsible for the dynamics observed at 480 nm and 500 nm vs 532 nm and 580 nm, i.e., spectral dependence of the relative cross sections seems to have an inflexion point at 500 nm, and (ii) the energy-transfer rates $\beta_{1,2}$ drop to half their values in going from $T=77$ K to 300 K (at both doping concentrations). One possible reason for the latter behavior is the proposed downward shift in energy of the LUMO level in the $Ir(DPPF)_3$ after a hole is trapped. The spectral overlap of the host emission and guest absorption is thus changed. The energy-transfer rate changes as well. A second reason is possible saturation of the Ir-complex sites available for energy transfer at $T=300$ K, since 35% of the guest population is occupied through charge trapping within the first picosecond after excitation.

IV. SUMMARY AND CONCLUSIONS

Gong and co-workers have recently reported[10–12,32] high-efficiency green electrophosphorescent light-emitting diodes (LED's) upon doping the PVK-PBD or conjugated copolymer hosts with $Ir(DPPF)_3$ or similar organometallic compounds. The devices exhibited no emission from PVK or PBD even at the lowest doping concentration of 0.1 wt %. These results indicate that Förster energy transfer plays minor role in achieving high efficiency in these devices, and that direct charge trapping is the dominant mechanism in electrophosphorescence. In the case of optical pumping, the situation is quite different. The PL spectra show that the emission of the host system is largely quenched only beyond 1 wt % doping of $Ir(DPPF)_3$. This behavior points to the long-range (dipole-dipole) Förster coupling as one of the major mechanisms responsible for energy transfer following photoexcitation in the phosphorescent blend.

We followed the leads from previous device work and approached this host/guest system with ultrafast spectroscopy technique. Determination of the sub-nanosecond dynamics of the excited-state populations in the blend is the key to quantify the rate and time scale of the energy transfer.

Time-resolved photoinduced absorption experiments on PVK-PBD blends (40 wt %) showed intriguing excited-state dynamics relative to the pristine PVK and PBD films. Examination of the host behavior (a blue emitter) at various probe wavelengths was essential for determining and subsequently modeling the energy-transfer mechanisms in the doped systems with small concentrations of $Ir(DPPF)_3$, which result in strong green phosphorescence.

We developed a model for the host system in which single excited-state species (primary excitations) and exciplexes contribute to the observed dynamics at low temperature ($T=77$ K). For short-wavelength probes, PVK excited species dominate the behavior observed in composites and thus the fitting parameters involved in data analysis, i.e., bimolecular decay rate and lifetime, resemble those obtained in pristine PVK films. The studies with longer-wavelength probes indicate an additional excited-state (exciplex) and that the overall decay is faster. The features of PBD excited species, i.e., fast bimolecular decay and short lifetime, as well as those from longer-lived PVK excited states were incorporated for modeling the composite host. Using the concerted effect of PVK and PBD primary excitations at these wavelengths, we defined new effective parameters, namely, the bimolecular decay rate and the natural lifetime. Simultaneously, as suggested by redshifted PL spectra from PVK-PBD blends, ex-

ciplexes are present. From fitting the data, we obtained an exciplex formation rate of $1/10\ \mathrm{ps}^{-1}$ and a lifetime of ~ 100 ps.

At room temperature, an additional time-independent term in the differential transmission curve was introduced to explain the time evolution of the excited population in the host. We have successfully applied the model of charge-trapping states, developed for conjugated polymer/fullerene blends,[21] to the PVK-PBD blends. We found that 35% of the primary photoexcitations evolve into CT states (either electron or hole trapping). Their relative cross sections at different wavelengths were inferred from fitting to the data. We note that the CT states in the host composite have an emissive character at 480 nm but become absorptive at longer probe wavelengths.

Finally, we performed pump-probe experiments in 0.2% and 2% $\mathrm{Ir(DPPF)_3}$ blends, at liquid-nitrogen and room temperatures. The HOMO and LUMO levels of the three components suggest that, upon excitation of PVK-PBD host, the charge carriers (electrons and holes) are trapped on the iridium complex where they eventually recombine. The remaining primary excitations undergo Förster-like energy transfer. Both the rate and the timing of the energy-transfer mechanism were found from the best-fit parameters to the experimental data. We attributed the slow energy transfer (over a time of at least 300 ps following the initial excitation) to the low oscillator strength of the guest absorption. The overall energy transfer is almost complete at room temperature in the 2 wt % blend, with a large contribution of 35% from CT states which exhibit emission at all probe wavelengths.

ACKNOWLEDGMENTS

The ultrafast spectroscopy was supported by the Air Force Office of Scientific Research under AFOSR Grant No. F49620-02-1-0127 (Charles Lee, Program Officer) and by the National Science Foundation under Grant No. NSF-DMR 0096820. The synthesis work was supported by the National Science Foundation under Grant No. CHE0098240. J. C. Ostrowski acknowledges support from the Eastman Kodak Company. R. A. Negres is grateful to Dr. V. Srdanov for valuable discussions.

*Corresponding author. Email address: ajh@physics.ucsb.edu

[1] M.A. Baldo, D.F. O'Brien, Y. You, A. Shoustikov, S. Sibley, M.E. Thompson, and S.R. Forrest, Nature (London) **395**, 151 (1998).
[2] M.A. Baldo, S. Lamansky, P.E. Burrows, M.E. Thompson, and S.R. Forrest, Appl. Phys. Lett. **75**, 4 (1999).
[3] M.A. Baldo, M.E. Thompson, and S.R. Forrest, Nature (London) **403**, 750 (2000).
[4] C. Adachi, M.A. Baldo, M.E. Thompson, and S.R. Forrest, J. Appl. Phys. **90**, 5048 (2001).
[5] T. Watanabe, E. Nakamura, S. Kawami, Y. Fukuda, T. Tsuji, T. Wakimoto, S. Miyaguchi, M. Yahiro, M.J. Yang, and T. Tsutsui, Synth. Met. **122**, 203 (2001).
[6] T. Tsutsui, M.J. Yang, M. Yahiro, K. Nakamura, T.W.T. Tsuji, Y. Fukuda, T. Wakimoto, and S. Miyaguchi, Jpn. J. Appl. Phys., Part 2 **38**, L1502 (1999).
[7] J.P.J. Markham, S.C. Lo, S.W. Magennis, P.L. Burn, and I.D.W. Samuel, Appl. Phys. Lett. **80**, 2645 (2002).
[8] A. Fukase, K.L.T. Dao, and J. Kido, Polym. Adv. Technol. **13**, 601 (2002).
[9] F.C. Chen, Y. Yang, M.E. Thompson, and J. Kido, Appl. Phys. Lett. **80**, 2308 (2002).
[10] X. Gong, M.R. Robinson, J.C. Ostrowski, D. Moses, G.C. Bazan, and A.J. Heeger, Adv. Mater. **14**, 581 (2002).
[11] X. Gong, J.C. Ostrowski, G.C. Bazan, D. Moses, and A.J. Heeger, Appl. Phys. Lett. **81**, 3711 (2002).
[12] X. Gong, J.C. Ostrowski, D. Moses, G.C. Bazan, and A.J. Heeger, Adv. Funct. Mater. **13**, 439 (2003).
[13] M. Ikai, S. Tokito, Y. Sakamoto, T. Suzuki, and Y. Taga, Appl. Phys. Lett. **79**, 156 (2001).
[14] T. Forster, Ann. Phys. (Leipzig) **2**, 55 (1948).
[15] T. Forster, Z. Naturforsch. A **4A**, 321 (1949).
[16] T. Forster, Discuss. Faraday Soc. **27**, 7 (1959).
[17] A. Dogariu, R. Gupta, A.J. Heeger, and H. Wang, Synth. Met. **100**, 95 (1999).
[18] G. Cerullo, S. Stagira, M. Zavelani-Rossi, S.D. Silvestri, T. Virgili, D.G. Lidzey, and D.D.C. Bradley, Chem. Phys. Lett. **335**, 27 (2001).
[19] J.C. Ostrowski, M.R. Robinson, A.J. Heeger, and G.C. Bazan, Chem. Commun. (Cambridge) **7**, 784 (2002).
[20] A. Dogariu, D. Vacar, and A.J. Heeger, Phys. Rev. B **58**, 10218 (1998).
[21] D. Vacar, E.S. Maniloff, D.W. McBranch, and A.J. Heeger, Phys. Rev. B **56**, 4573 (1997).
[22] E.S. Maniloff, V.I. Klimov, and D.W. McBranch, Phys. Rev. B **56**, 1876 (1997).
[23] R.G. Kepler, V.S. Valencia, S.J. Jacobs, and J.J. McNamara, Synth. Met. **78**, 227 (1996).
[24] G.J. Denton, N. Tessler, N.T. Harrison, and R.H. Friend, Phys. Rev. Lett. **78**, 733 (1997).
[25] M. Pope and C. E. Swenberg, *Electronic Processes in Organic Crystals and Polymers*, 2nd ed. (Oxford University Press, New York, 1999), Chap. VI, pp. 646–773, and references therein.
[26] X. Jiang, R.A. Register, K.A. Killeen, M.E. Thompson, F. Pschenitzka, T.R. Hebner, and J.C. Sturm, J. Appl. Phys. **91**, 6717 (2002).
[27] N.S. Sariciftci, L. Smilowitz, A.J. Heeger, and F. Wudl, Science **258**, 1474 (1992).
[28] B. Kraabel, J.C. Hummelen, D. Vacar, D. Moses, N.S. Sariciftci, A.J. Heeger, and F. Wudl, J. Chem. Phys. **104**, 4267 (1996).
[29] B. Kraabel, D. McBranch, N.S. Sariciftci, D. Moses, and A.J. Heeger, Phys. Rev. B **50**, 18543 (1994).
[30] Z.-L. Zhang, X.-Y. Jiang, S.-H. Xu, and T. Nagatomo, in *Organic Electroluminescent Materials and Devices*, edited by S. Miyata and H. S. Nalwa (Gordon and Breach, Amsterdam, 1997), pp. 203–230.
[31] M.G. Colombo, A. Hauser, and H.U. Gudel, Top. Curr. Chem. **171**, 143 (1994), and references therein.
[32] X. Gong, J.C. Ostrowski, G.C. Bazan, D. Moses, A.J. Heeger, M.S. Liu, and A.K.-Y. Jen, Adv. Mater. **15**, 45 (2003).